

Low bandgap polymers synthesized by FeCl₃ oxidative polymerization

Tianqi Cai^{a,c}, Yi Zhou^b, Ergang Wang^{a,*}, Stefan Hellström^a, Fengling Zhang^b, Shiai Xu^c, Olle Inganäs^b, Mats R. Andersson^{a,b,**}

^a Materials and Surface Chemistry/Polymer Technology, Chalmers University of Technology, SE-412 96 Göteborg, Sweden

^b Biomolecular and Organic Electronics, IFM, and Centre of Organic Electronics, Linköping University, SE-581 83 Linköping, Sweden

^c School of Materials Science and Engineering, East China University of Science and Technology, Meilong Road 130, 200237 Shanghai, China

ARTICLE INFO

Article history:

Received 1 December 2009

Received in revised form

17 March 2010

Accepted 20 March 2010

Available online 10 April 2010

Keywords:

Polymer solar cells

Bulk heterojunction

FeCl₃ oxidative polymerization

Low bandgap polymers

Benzo[c][1,2,5]thiadiazole

ABSTRACT

Four low bandgap polymers, combining an alkyl thiophene donor with benzo[c][1,2,5]thiadiazole, 2,3-diphenylquinoxaline, 2,3-diphenylthieno[3,4-b]pyrazine and 6,7-diphenyl-[1,2,5]thiadiazolo[3,4-g]quinoxaline acceptors in a donor–acceptor–donor architecture, were synthesized via FeCl₃ oxidative polymerization. The molecular weights of the polymers were improved by introducing *o*-dichlorobenzene (ODCB) as the reaction solvent instead of the commonly used solvent, chloroform. The photophysical, electrochemical and photovoltaic properties of the resulting polymers were investigated and compared. The optical bandgaps of the polymers vary between 1.0 and 1.9 eV, which is promising for solar cells. The devices spin-coated from an ODCB solution of P1DB:[70]PCBM showed a power conversion efficiency of 1.08% with an open-circuit voltage of 0.91 V and a short-circuit current density of 3.36 mA cm⁻² under irradiation from an AM1.5G solar simulator (100 mW cm⁻²).

© 2010 Elsevier B.V. All rights reserved.

1. Introduction

With increasing energy demand, polymer-based solar cells have been attracting considerable attention for their unique advantages, such as low cost, light weight, and potential use in flexible devices [1–5]. As a result, the development of polymer solar cells has increased rapidly, yielding power conversion efficiencies (PCEs) up to 5–6% [6–11]. In order to produce cheaper electricity, the PCEs of polymer solar cells need further improvement. One of the limiting parameters for PCE of polymer solar cells is the mismatch between the absorption spectrum of the photoactive layer and the terrestrial solar radiation, which leads to only a small portion of solar energy being utilized. Low bandgap polymers ($E_g < 1.8$ eV) are of interest because their absorption spectra can cover from the visible to the near-infrared region, and have been intensively investigated [12–15]. By using solar cells fabricated from low bandgap polymers, it is possible to capture more of the solar radiation and thereby increase their efficiency. A facile approach to achieve low bandgap polymers is through incorporation of electron-rich units (as donor) with electron-deficient units (as acceptor), forming a donor–acceptor

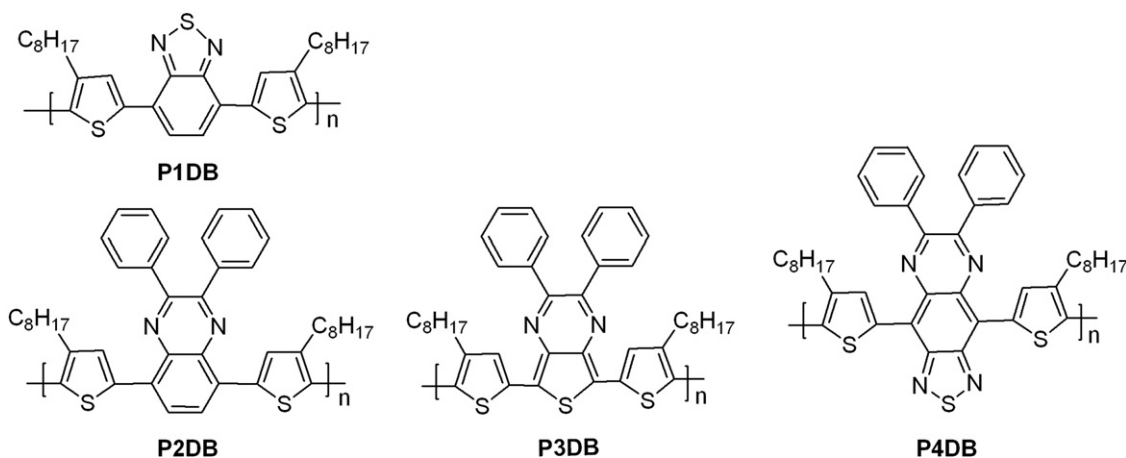
(D–A) structure [16–19]. The interaction between electron-rich units and electron-deficient units results in a compressed bandgap, which can be tuned conveniently by changing one of the units or both of them.

Most low bandgap polymers were synthesized via Suzuki [20–22], Yamamoto [22] and Stille [23,24] coupling polymerizations. Compared with these polymerization methods, ferric(III) chloride (FeCl₃) oxidative polymerization is easy and cheap with mild reaction conditions (at room temperature), thereby making it suitable for large scale production [25]. Here we present four low bandgap polymers that combine an alkyl thiophene donor with four different electron-deficient acceptors. The use of a donor–acceptor–donor (DAD) monomer architecture allows for synthesis via FeCl₃ oxidative polymerization (See Scheme 1). Similar polymers to P1DB have been reported [26,27], and will be compared in this paper. Octyl groups were attached at the 4 position of the thiophene moiety to increase the solubility of the resulting polymers. Benzo[c][1,2,5]thiadiazole, 2,3-diphenylquinoxaline, 2,3-diphenylthieno[3,4-b]pyrazine and 6,7-diphenyl-[1,2,5]thiadiazolo[3,4-g]quinoxaline were used as acceptor units in the alternating polymers. The influence of the acceptor units on photophysical, electrochemical and photovoltaic properties of the resulting polymers were investigated and compared. To improve the molecular weights of the polymers, *o*-dichlorobenzene (ODCB) was used as the reaction solvent instead of the commonly used solvent, chloroform. As a result, the polymers had improved molecular weights due to their higher solubility in ODCB compared to chloroform.

* Corresponding author. Tel.: +46 31 7723401; fax: +46 31 7723418.

** Corresponding author at: Materials and Surface Chemistry/Polymer Technology, Chalmers University of Technology, SE-412 96 Göteborg, Sweden. Tel.: +46 31 7723401; fax: +46 31 7723418.

E-mail addresses: ergang@chalmers.se (E. Wang), mats.andersson@chalmers.se (M.R. Andersson).



Scheme 1. The chemical structures of the synthesized polymers.

2. Experimental

2.1. Materials

All reagents were purchased from Aldrich except for the following chemicals: 3-octylthiophene, benzo[*c*][1,2,5]thiadiazole, 2,5-dibromo-3,4-dinitrothiophene, which were bought from Puyang Huicheng Chemical co. Dry tetrahydrofuran (THF) was distilled over sodium with addition of benzophenone. All reactions were performed under nitrogen unless noted.

2.2. Synthesis of monomers

2.2.1. Tributyl(4-octylthiophen-2-yl)stannane (**1**)

Butyl-lithium in hexane (1.6 mol L^{-1} , 63 mL, 0.10 mol) was slowly added to 3-octylthiophene (19.60 g, 0.10 mol) in anhydrous THF (150 mL) at -80°C , after which the mixture was stirred under nitrogen for 1.5 h. After increasing to room temperature for 1 h, the mixture was then cooled to -80°C and tributylchlorostannane (35.50 g, 0.11 mol) was added dropwise. The mixture was then stirred at -80°C for an additional 1 h, followed by quenching with 2 M aqueous sodium hydrogen carbonate (100 mL). After that, most of THF was removed under reduced pressure and the solution was extracted with diethyl ether. The organic phase was separated and washed with 2 M aqueous sodium hydrogen carbonate (150 mL \times 3) and brine (50 mL \times 3). The organic phase was dried over MgSO_4 . After removing the solvents, the residue was purified on a column of neutral alumina (hexane as eluent) to give the compound (**1**) as colorless oil (37.00 g, 76.3%). It was used in the next step without further purification.

2.2.2. 4,7-Dibromobenzo[*c*][1,2,5]thiadiazole (**2**)

After a mixture of 2,1,3-benzothiadiazole (20.00 g, 147 mmol) and aq. HBr (48%, 300 mL) was heated to reflux under N_2 , Br_2 (70.50 g, 441 mmol, dissolved in 200 mL of 48% aq. HBr) was added dropwise over 1 h. The mixture was refluxed for an additional 6 h. After the reaction, 1 M $\text{Na}_2\text{S}_2\text{O}_3$ solution was slowly added until the orange solution turned to yellow. The solid was filtrated and washed with distilled water (100 mL \times 3). The solid was recrystallized in ethanol to yield compound **2** as yellow crystals (30.10 g, 69.3%). $^1\text{H NMR}$ (400 MHz, CDCl_3) δ : 7.71 (s, 2 H). $^{13}\text{C NMR}$ (100 MHz, CDCl_3) δ : 153.08, 132.50, 114.05.

2.2.3. 4,7-Bis(4-octylthiophen-2-yl)benzo[*c*][1,2,5]thiadiazole (**3**)

To the solution of **1** (11.78 g, 24.3 mmol) and **2** (2.95 g, 10.0 mmol) in THF (50 mL) was added $\text{Pd}(\text{PPh}_3)_2\text{Cl}_2$ (75 mg,

0.11 mmol). The mixture was refluxed overnight under nitrogen. The THF was then removed under reduced pressure, and the residue was extracted with CH_2Cl_2 and washed by water. The organic phase was separated and dried over MgSO_4 . After purification by chromatography using CH_2Cl_2 :hexane=1:1 as the eluent and recrystallization from ethanol, compound **3** was obtained as orange crystals (2.21 g, 42%). $^1\text{H NMR}$ (400 MHz, CDCl_3) δ : 7.98 (s, 2 H), 7.83 (s, 2 H), 7.04 (s, 2 H), 2.71–2.68 (t, 4 H), 1.72–1.69 (m, 4 H), 1.40–1.29 (m, 20 H), 0.89–0.87 (t, 6 H). $^{13}\text{C NMR}$ (100 MHz, CDCl_3) δ : 152.86, 144.60, 139.24, 129.23, 126.24, 125.76, 121.77, 32.18, 30.93, 30.79, 29.74, 29.67, 29.57, 22.96, 14.41.

2.2.4. 5,8-Bis(4-octylthiophen-2-yl)-2,3-diphenylquinoxaline (**4**)

Compound **3** (1.43 g, 2.72 mmol) was mixed with zinc (1.17 g, 18.0 mmol) in a flask and 50 mL acetic acid was added. The reaction was stirred at 60°C for 6 h. Upon cooling to room temperature, the solid residue was removed by filtration and then benzil (0.87 g, 4.14 mmol) was added to the solution at once. The mixture was heated to 40°C and stirred overnight. Then the mixture was poured into water and extracted with CH_2Cl_2 (50 mL \times 3). The organic phase was separated and dried over MgSO_4 , and then purified by column chromatography using CH_2Cl_2 :hexane=1:1 as the eluent. Recrystallization from ethanol yielded compound **4** as orange crystals (1.51 g, 82.7%). $^1\text{H NMR}$ (400 MHz, CDCl_3) δ : 8.09 (s, 2 H), 7.76 (s, 2 H), 7.74 (s, 4 H), 7.38 (s, 4 H), 7.37 (s, 2 H), 7.11 (s, 2 H), 2.70–2.66 (t, 4 H), 1.74–1.67 (m, 4 H), 1.40–1.29 (m, 20 H), 0.90–0.87 (t, 6 H). $^{13}\text{C NMR}$ (100 MHz, CDCl_3) δ : 151.55, 142.94, 138.86, 138.54, 137.38, 131.33, 130.61, 129.07, 128.31, 128.17, 127.01, 123.93, 32.09, 30.08, 30.75, 29.69, 29.60, 29.47, 22.86, 14.31.

2.2.5. 2,5-Bis(3-octylthiophene-5-yl)-3,4-dinitrothiophene (**5**)

To the solution of 2,5-dibromo-3,4-dinitrothiophene (3.98 g, 11.70 mmol) and compound **1** (12.80 g, 26.40 mmol) in 60 mL THF was added $\text{Pd}(\text{PPh}_3)_2\text{Cl}_2$ (0.09 g, 0.13 mmol). The mixture was refluxed overnight. After the reaction, THF was removed under reduced pressure, and the residue was extracted by CH_2Cl_2 (60 mL \times 3) and washed by water (60 mL \times 3). The organic phase was separated and dried over MgSO_4 . After purification by column chromatography using CH_2Cl_2 :hexane=1:1 as the eluent and recrystallization from ethanol, compound **5** was obtained as an orange powder (3.89 g, 59.0%). $^1\text{H NMR}$ (400 MHz, CDCl_3) δ : 7.36 (s, 2 H), 7.18 (s, 2 H), 2.64–2.60 (t, 4 H), 1.63–1.61 (m, 4 H), 1.31–1.28 (m, 20 H), 0.90–0.87 (t, 6 H). $^{13}\text{C NMR}$ (100 MHz, CDCl_3)

δ : 145.18, 134.23, 132.52, 128.01, 126.29, 115.18, 32.11, 30.61, 30.54, 29.62, 29.48, 22.92, 14.37.

2.2.6. 5,7-Bis(4-octylthiophen-2-yl)-2,3-diphenylthieno [3,4-*b*]pyrazine (**6**)

Compound **5** (1.02 g, 1.8 mmol) was mixed with iron powder (2.20 g, 39.3 mmol) in a flask and 50 mL acetic acid was added. The mixture was stirred at 60 °C for 1 h. After the solution cooled to room temperature, the solid residue was removed by filtration and then benzil (0.62 g, 2.95 mmol) was added to the solution at once. The mixture was heated to 60 °C, and stirred overnight. The mixture was then poured into water and extracted with CH₂Cl₂ (50 mL \times 3). The organic phase was separated and dried over MgSO₄, and then purified by column chromatography using CH₂Cl₂:hexane=1:3 as the eluent. Recrystallization from ethanol yielded compound **6** as a purple powder (0.65 g, 53.3%). ¹H NMR (400 MHz, CDCl₃) δ : 7.60–7.58 (m, 4 H), 7.49 (s, 2 H), 7.38–7.31 (m, 6 H), 6.98 (s, 2 H), 2.66–2.62 (t, 4 H), 1.70–1.64 (m, 4 H), 1.42–1.28 (m, 20 H), 0.91–0.87 (t, 6 H). ¹³C NMR (100 MHz, CDCl₃) δ : 152.77, 143.66, 139.22, 137.52, 134.40, 130.15, 129.10, 128.16, 126.06, 125.07, 121.84, 115.17, 32.07, 30.62, 29.63, 29.50, 29.44, 22.86, 14.30.

2.2.7. 4,9-Dibromo-6,7-diphenyl-[1,2,5]thiadiazolo [3,4-*g*]quinoxaline (**7**)

4,7-Dibromo-5,6-dinitrobenzo[c][1,2,5]thiadiazole (3.89 g, 10.1 mmol) was mixed with iron powder (11.7 g, 208.9 mmol) in a flask and then 350 mL acetic acid was added. The reaction was heated at reflux for 1 h. Upon cooling to room temperature, the solid residue was removed by filtration and then benzil (3.42 g, 16.3 mmol) was added to the solution at once. Then the mixture was heated to 60 °C, and stirred overnight. The mixture was then poured into water and extracted with CH₂Cl₂ (50 mL \times 3). The organic phase was separated and dried over MgSO₄, and then purified by column chromatography using CH₂Cl₂:hexane=1:1 as the eluent. Recrystallization from ethanol yielded compound **7** as red crystals (2.65 g, 53.2%). ¹H NMR (400 MHz, CDCl₃) δ : 7.75–7.73 (d, 4 H), 7.50–7.46 (t, 2 H), 7.42–7.39 (t, 4 H). ¹³C NMR (100 MHz, CDCl₃) δ : 156.24, 152.56, 138.28, 137.78, 130.65, 130.50, 128.66, 114.41.

2.2.8. 4,9-Bis(4-octylthiophen-2-yl)-6,7-diphenyl-[1,2,5]thiadiazolo[3,4-*g*]quinoxaline (**8**)

To the solution of **7** (2.60 g, 5.2 mmol) and **1** (6.07 g, 12.5 mmol) in 25 mL THF was added Pd(PPh₃)₂Cl₂ (0.158 g, 0.23 mmol). The reaction was refluxed overnight. THF was then removed under reduced pressure, and the residue was extracted with CH₂Cl₂ (50 mL \times 3) and washed with water (100 mL \times 3). The organic phase was dried over MgSO₄ and purified by column chromatography using CH₂Cl₂:hexane=1:3 as the eluent. Recrystallization from ethanol yielded compound **8** as a green solid (2.10 g, 55.4%). ¹H NMR (300 MHz, CDCl₃) δ : 8.85 (s, 2 H), 7.82–7.80 (d, 4 H), 7.44–7.39 (m, 6 H), 7.29 (s, 2 H), 2.79–2.76 (t, 4 H), 1.78–1.74 (m, 4 H), 1.40–1.29 (m, 20 H), 0.90–0.87 (t, 6 H). ¹³C NMR (100 MHz, CDCl₃) δ : 153.07, 151.96, 143.15, 138.35, 135.77, 134.96, 134.90, 130.92, 129.72, 128.39, 127.01, 121.36, 32.21, 30.92, 29.82, 29.77, 29.63, 22.98, 14.42.

2.3. Synthesis of polymers

All of the polymers were synthesized in chloroform (CF) and ODCB, respectively, and the corresponding polymers were named PnCF and PnDB ($n=1-4$), respectively. Both CF and ODCB were bubbled with N₂ for 30 min before use. The same molar ratio of FeCl₃ to monomer (5:1) was used in each case with the exception

of P2DB, which did not dissolve well in ODCB after purification. The polymer was then synthesized again with a reduced ratio of FeCl₃ to monomer in order to limit the molecular weight and increase the solubility.

2.3.1. Poly[4,7-Bis(3-octylthiophene-5-yl)benzo-2,1,3-thiadiazole] in chloroform (P1CF)

To a suspension of FeCl₃ (400 mg, 2.47 mmol) in chloroform (5 mL), compound **3** (280 mg, 0.53 mmol) in chloroform (4 mL) was added in one portion under N₂. The reaction was stirred for 48 h at room temperature. After that, the mixture was diluted by chloroform and washed by water. Then the organic phase was separated and stirred with ammonia (aq. 20%, 200 mL \times 2) for 12 h, and then washed with 0.2 M ethylenediaminetetraacetic acid (EDTA) solution (200 mL \times 2) and water (200 mL \times 2). The solution was then poured into methanol and the precipitate was collected by filtration. The crude material was purified via Soxhlet with diethyl ether and chloroform. The chloroform solution was then precipitated into methanol and collected by filtration. The polymer was obtained as a red solid (124 mg, 44.3%).

2.3.2. Poly[4,7-Bis(3-octylthiophene-5-yl)benzo-2,1,3-thiadiazole] in ODCB (P1DB)

To a suspension of FeCl₃ (240 mg, 1.5 mmol) in ODCB (3 mL), compound **3** (160 mg, 0.3 mmol) in ODCB (3 mL) was added in one portion under N₂. The reaction was left stirring for 24 h at room temperature. The reaction mixture was then diluted with ODCB and washed with water. The organic phase was then separated and stirred with ammonia (aq. 20%, 200 mL \times 2) for 12 h, followed by washing with 0.2 M EDTA solution (200 mL \times 2) and water (200 mL \times 2). The solution was then poured into methanol and the precipitate was collected by filtration. The crude material was purified via Soxhlet with diethyl ether and chloroform. The chloroform solution was then precipitated into methanol. After filtration, the polymer was obtained as a red solid (89 mg, 56.0%).

2.3.3. Poly[5,8-bis(4-octylthiophen-2-yl)-2,3-diphenylquinoxaline] in chloroform (P2CF)

P2CF was synthesized by following the same procedure used in Section 2.3.1. After Soxhlet, some solid was left in the thimble, most of which did not dissolve in ODCB. As a result, the yield of this polymer is quite low (12.5%).

2.3.4. Poly[5,8-bis(4-octylthiophen-2-yl)-2,3-diphenylquinoxaline] in dichlorobenzene (P2DB)

P2DB was synthesized by following the same procedure used in Section 2.3.2. After Soxhlet with diethyl ether, the solid residue in the thimble was dissolved in ODCB and filtered through a glass filter and then precipitated into methanol. The polymer was obtained as a red solid by collecting with PTFE filter (yield: 20.0%).

2.3.5. Poly[5,7-bis(4-octylthiophen-2-yl)-3-diphenylthieno [3,4-*b*]pyrazine] in chloroform (P3CF)

P3CF was synthesized by following the same procedure used in Section 2.3.1. After purification, the polymer was obtained as a green solid (yield: 40%).

2.3.6. Poly[5,7-bis(4-octylthiophen-2-yl)-2,3-diphenylthieno [3,4-*b*]pyrazine] in ODCB (P3DB)

P3DB was synthesized by following the same procedure used in Section 2.3.2. After purification, the polymer was obtained as a green solid (yield: 53%).

2.3.7. Poly[4,9-bis(4-octylthiophen-2-yl)-6,7-diphenyl-1,2,5]thiadiazolo[3,4-g]quinoxaline] in chloroform (P4CF)

P4CF was synthesized by following the same procedure used in Section 2.3.1. After purification, the polymer was obtained as a green solid (yield: 42%).

2.3.8. Poly[4,9-bis(4-octylthiophen-2-yl)-6,7-diphenyl-1,2,5]thiadiazolo[3,4-g]quinoxaline] in ODCB (P4DB)

P4DB was synthesized by following the same procedure used in Section 2.3.2. After purification, the polymer was obtained as a green solid (yield: 28%).

2.4. Measurements

¹H-NMR and ¹³C-NMR spectra were acquired from a Varian 300 MHz and a Bruker Avance 400 MHz spectrophotometer. Tetramethylsilane were used as an internal reference with deuterated chloroform as solvent. Size exclusion chromatography (SEC) was performed on Waters Alliance GPCV2000 with a refractive index detector columns: Waters Styvigel HT GE × 1, Waters Styvigel HMW GE × 2. The eluent was 1,2,4-trichlorobenzene. The working temperature was 135 °C and the resolution time was 2 h. The concentration of the samples was 0.5 mg mL⁻¹, which was filtered (filter: 0.45 μm) prior to the analysis. The molecular weights were calculated according relative calibration with polystyrene standards. UV–vis absorption spectra were measured with a Perkin Elmer Lambda 900 UV–vis-NIR absorption spectrometer. Square-wave voltammetry (SWV) measurements were carried out on a CH-Instruments 650A Electrochemical Workstation. A three-electrode setup was used with platinum wires both as working electrode and counter electrode, and Ag/Ag⁺ used as reference electrode calibrated with Fc/Fc⁺. A 0.1 M solution of tetrabutylammonium hexafluorophosphate (Bu₄NPF₆) in anhydrous acetonitrile was used as supporting electrolyte. The polymers were deposited (together with a small amount of the Bu₄NPF₆) onto the working electrode from ODCB solution. In order to remove oxygen from the electrolyte, the system was bubbled with nitrogen prior to each experiment. The nitrogen inlet was then moved to above the liquid surface and left there during the scans.

2.5. Fabrications of solar cell devices

The structure of the solar cell is Glass/ITO/PEDOT:PSS/Active Layer/LiF/Al, which were fabricated by spin-coating. As a buffer layer, the conductive polymer PEDOT:PSS (Baytron P VP Al 4083) was spin-coated onto ITO-coated glass substrates, followed by annealing at 120 °C for 5 min to remove water. The active layer of mixed polymers and [6,6]-phenyl-C71-butyric acid methyl ester ([70]PCBM) was spin-coated from ODCB solution onto the PEDOT:PSS layer. LiF (0.6 nm) and Al (60 nm) were used as top electrodes and were deposited in vacuum onto the active layer. The size of the diode was defined by a mask when depositing Al in vacuum, and was approximately 5 mm². The external quantum efficiencies (EQEs) were calculated from the photocurrents at short-circuits conditions. The currents were recorded by a Keithley 485 picoammeter under illumination of monochromatic light through the ITO side of the devices. Power conversion efficiencies were measured under an AM1.5G solar simulator (100 mW cm⁻², Model SS-50A, Photo Emission Tech., Inc.).

3. Results and discussions

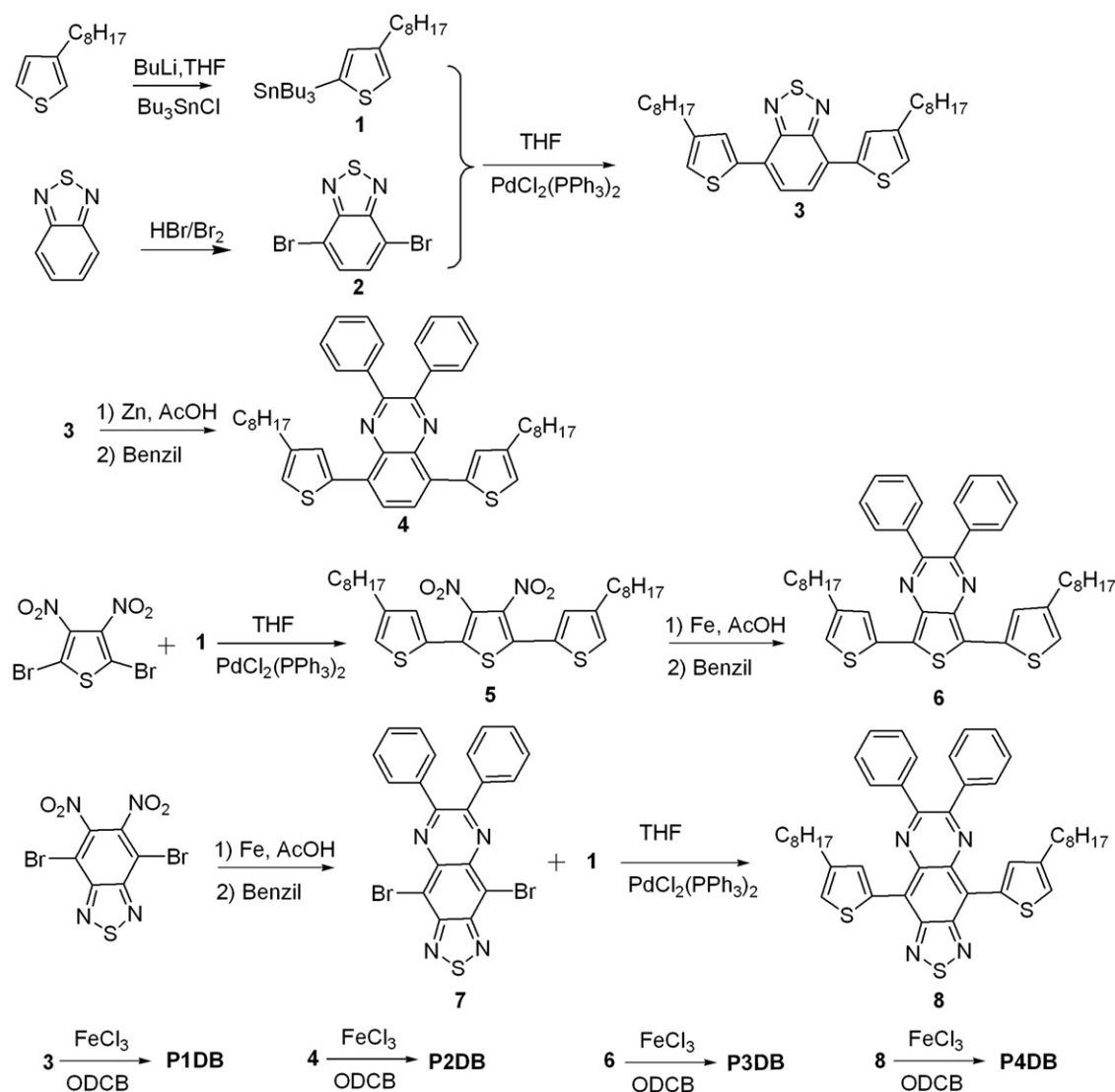
3.1. Synthesis and characterization

A series of DAD conjugated polymers have been synthesized via FeCl₃ oxidative polymerization in chloroform and ODCB, respectively. The synthetic routes for the monomers and polymers are summarized in Scheme 2 and the molecular weights of the polymers can be seen in Table 1. Monomer **3** was obtained via Stille coupling of 4,7-dibromobenzo[c][1,2,5]thiadiazole and tributyl(4-octylthiophen-2-yl)stannane. The reduction of compound **3** with zinc in acetic acid gave the diamine compound, which was then condensed with benzil affording monomer **4**. Stille coupling of 2,5-dibromo-3,4-dinitrothiophene and tributyl(4-octylthiophen-2-yl)stannane yielded **5**, which was reduced by iron in acetic acid and condensed with benzil to afford monomer **6**. 4,7-Dibromo-5,6-dinitrobenzo[c][1,2,5]thiadiazole was reduced by iron and condensed with benzil yielding compound **7** as a red powder. Compound **7** and tributyl(4-octylthiophen-2-yl)stannane were combined via Stille coupling to afford monomer **8**. Firstly, all four monomers were polymerized in the commonly used solvent chloroform, with FeCl₃ as an oxidant. As shown in Table 1, the molecular weights of the resulting polymers are not high, which can be attributed to the poor solubility of the polymers. It was observed that the polymers precipitated gradually from the reaction solution during the polymerization. According to the mechanism of FeCl₃ oxidative polymerization [25], the oxidized polymer chains were complexed with FeCl₄⁻ counter ions while growing, which reduced the solubility of the polymers. In order to improve the molecular weights of the polymers, ODCB was used as the reaction solvent instead of chloroform, due to its increased soluble effect for the following polymers. Using the new solvent, the molecular weights of these polymers were improved while the polydispersities (PDI) of P2DB, P3DB and P4DB were reduced. Comparing PB4TB (the same structure as P1DB) to P1DB, which was synthesized by Janssen's group via FeCl₃ oxidative polymerization in chloroform giving an *M_n* of 15,500 and *M_w* of 42,200 [26], is slightly lower than the molecular weight obtained for P1DB with ODCB as the reaction solvent.

One of the difficulties of the FeCl₃ polymerization is the removal of the iron salts after polymerization, since a minute amount of metal residue will influence the resulting device performance [28,29]. Here, for purification, we used ammonia and EDTA solutions to wash the polymer solutions, since the complex of the iron ion with the ammonium salt can be dissolved in water and then removed. The polymer purified by washing with ammonia and EDTA solutions showed a much better performance compared to the one without purification.

3.2. Optical and electrochemical measurements

The solution and solid state UV–vis absorption spectra for the polymers can be seen in Fig. 1. All of the polymers showed two distinct absorption bands: the band around 300–400 nm can be assigned to the π–π* transition while the long-wavelength absorption peaks can be attributed to intramolecular charge transfer between the thiophene donor and the acceptor moieties [30,31]. The absorption spectra of the polymers in solid state are red shifted compared to the corresponding spectra in solution, which can be attributed to an increase in the aggregate conformation formed in the solid state. P3DB exhibited a significant absorption into the near-infrared region. The maximum absorption of P3DB is located at ca. 700 nm, which is the highest photon flux of solar radiation, thus more photons are



Scheme 2. The synthetic routes for the monomers and polymers.

Table 1
The molecular weights of the polymers.

| Polymer | Reaction solvent | M_n | M_w | PDI |
|---------|------------------|---------|-----------|------|
| P1CF | Chloroform | 8500 | 21,000 | 2.5 |
| P1DB | ODCB | 26,000 | 102,000 | 3.9 |
| P2CF | Chloroform | 5800 | 44,000 | 7.5 |
| P2DB | ODCB | 9400 | 17,000 | 1.8 |
| P3CF | Chloroform | 15,000 | 240,000 | 15.5 |
| P3DB | ODCB | 22,700 | 212,000 | 9.3 |
| P4CF | Chloroform | 14,000 | 1400,000 | 100 |
| P4DB | ODCB | 226,000 | 9,600,000 | 42.3 |

expected to be absorbed by this material. P4DB showed a strong absorption in the near-infrared, peaking at 884 nm in the solid state, which is blue-shifted compared to PBTQ reported by Zoombelt et al. [32]. The blue-shift can be attributed to the twist between the head-to-head linked alkylthiophenes in P4DB. The optical bandgaps of the polymers were deduced from the onset of absorption in the solid state, and vary between 1.0 and 1.9 eV, which is promising for solar cell applications. The absorption maximum and optical bandgaps (E_g^{op}) of the polymers are summarized in Table 2.

The HOMO (highest occupied molecular orbital)/LUMO (lowest unoccupied molecular orbital) levels of the polymers are important parameters for investigating their photovoltaic performance. These levels can be estimated using electrochemistry. The polymers were investigated by SWV and the related voltammograms are shown in Fig. 2. For comparison, [60]PCBM was also measured under the same conditions, which showed a peak oxidation potential at 1.45 V and a peak reduction potential at -1.08 V. According to the data summarized in Table 2, the offset of the LUMO levels between the polymers P1DB, P2DB, P3DB and [60]PCBM is larger than 0.3 eV, which indicates there is enough driving force for charge separation in their solar cells [15]. The high ionization potential of P1DB is in favor of achieving a high open-circuit voltage (V_{oc}) in the resulting devices [15]. The reduction potential of P4DB (-1.16 V) is very close to that of [60]PCBM (-1.08 V), which might decrease the solar cell performance due to the insufficient driving force for exciton dissociation.

3.3. Photovoltaic studies

All four polymers were investigated in solar cells with a sandwich configuration of Glass/ITO/PEDOT:PSS/Active layer/LiF/Al. The active layer of the solar cells were spin-coated from chloroform

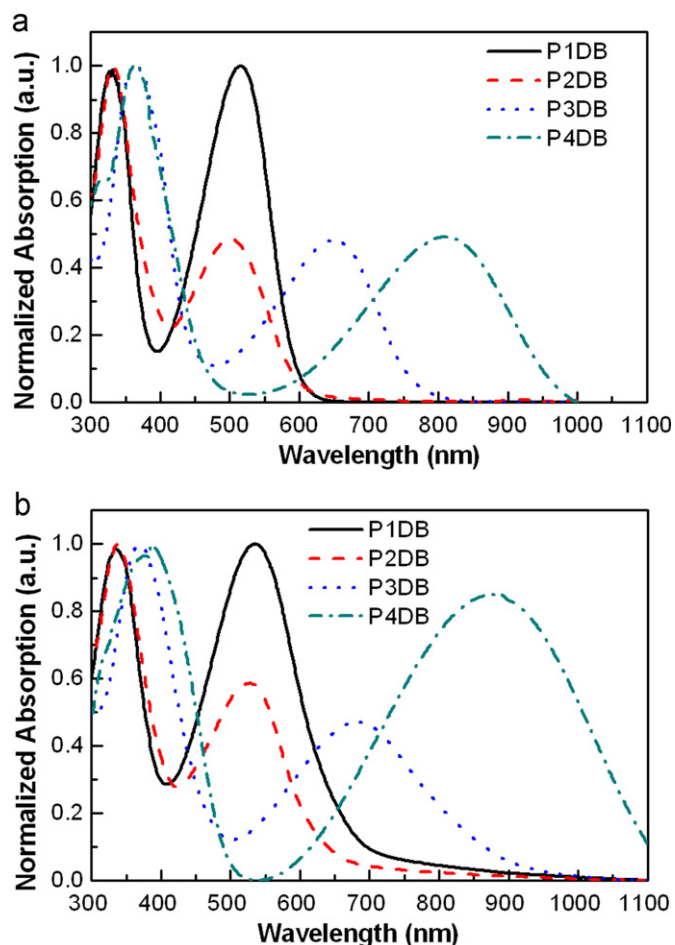


Fig. 1. UV-vis absorption spectra of the polymers (a) in solution and (b) in the solid state.

Table 2
The optical and electrochemical data of the polymers.

| Polymer | λ_{\max} (nm) | | λ_{onset} (nm) | E_g^{op} (eV) | E^{ox} (V) | E^{red} (V) | E_g^{ec} (eV) |
|---------|-----------------------|---------|-------------------------------|------------------------|---------------------|----------------------|------------------------|
| | Solution | Film | Film | | | | |
| P1DB | 331,515 | 335,536 | 696 | 1.78 | 0.70 | -1.71 | 2.41 |
| P2DB | 333,501 | 338,527 | 658 | 1.88 | 0.55 | -1.82 | 2.37 |
| P3DB | 368,651 | 370,682 | 930 | 1.33 | 0.33 | -1.57 | 1.90 |
| P4DB | 363,810 | 385,884 | 1200 | 1.00 | 0.48 | -1.16 | 1.64 |

solutions of polymer:[60]PCBM (the optimized ratio is 1:4, wt%) with [60]PCBM as the electron acceptor. Due to the poor solubility of P2DB in chloroform, no solar cell data could be obtained. It is reported that the V_{oc} linearly correlates to the energy difference between the HOMO of the donor and the LUMO of the acceptor [15]. The devices from P1DB showed the highest V_{oc} of 1.04 V, which is in accordance with its high oxidation potential [15]. Conversely, P3DB showed a low V_{oc} of 0.55 V, due to its low oxidation potential. As indicated by the low reduction potential of P4DB, the devices from P4DB:[60]PCBM gave a very poor performance.

Considering that the asymmetric structure of [70]PCBM can absorb more solar radiation than [60]PCBM [33,34], [70]PCBM was also used as an electron acceptor to improve the performance of the solar cells in combination with ODCB as the solvent. P2DB was also tested, since its solubility in ODCB is better than in chloroform. The

J - V characteristics of the devices from polymer:[70]PCBM and P1DB:[60]PCBM are shown in Fig. 3 and the V_{oc} , short-circuit current density (J_{sc}), fill factor (FF) and PCE data are summarized in Table 3. To confirm the device performance, external quantum efficiencies (EQEs) from the cells of polymer:[70]PCBM were measured under monochromatic light and the EQE profiles can be seen in Fig. 4. As expected, an obvious improvement in performance for all polymers was observed with [70]PCBM as an electron acceptor. In this case, the J_{sc} of the cells from P1DB and P3DB increased at least 1 mA cm^{-2} (Table 3), which is also confirmed by the obviously enhanced intensity of their EQE profiles (see Fig. 4). The cells from P1DB:[70]PCBM gave the highest PCE of 1.08%, and benefited from a reasonably high V_{oc} of 0.91 V. Although the efficiencies of the cells from P3DB were low, limited by its low V_{oc} , the J_{sc} is reasonably high due to its broad absorption spectrum. It's not clear why the cells from P2DB showed an even lower V_{oc} than that of P3DB, even though the oxidation potential of P2DB is higher than that of P3DB. The poor solubility and low molecular weight ($M_n=9000$) of P2DB may be the main reasons.

4. Conclusion

Four low bandgap polymers that combine an alkyl thiophene donor with different electron-deficient units forming a DAD structures were synthesized via FeCl_3 oxidative polymerization with chloroform and ODCB as solvents. The devices spin-coated

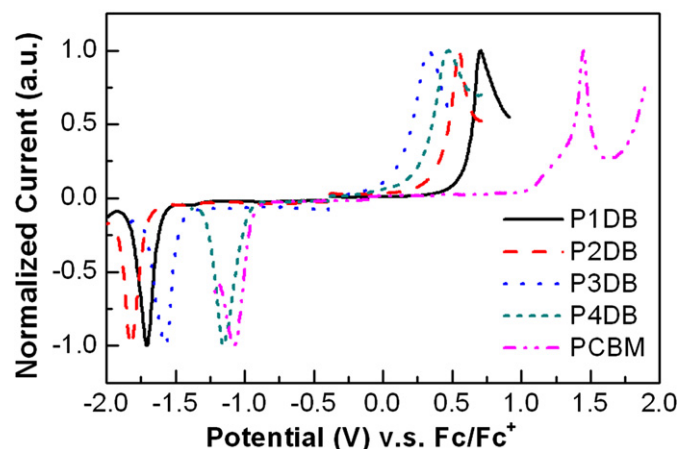


Fig. 2. SWV measurements of the polymers and [60]PCBM in film.

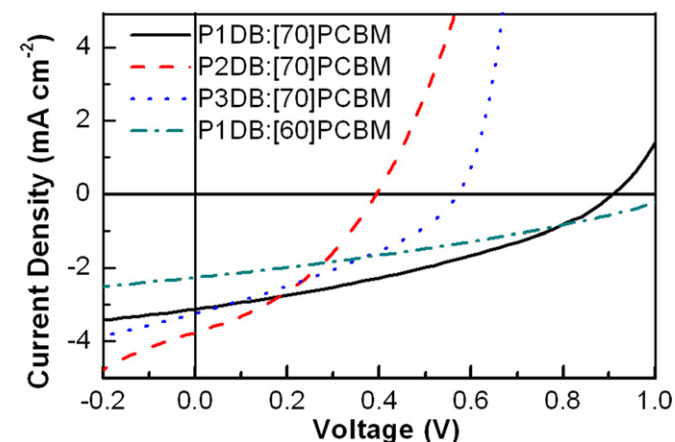


Fig. 3. J - V characteristics of the devices from polymer:[70]PCBM and P1DB:[60]PCBM.

Table 3
Photovoltaic properties of the devices prepared from the polymers.

| Polymer | Polymer:PCBM (wt%) | J_{sc} (mA cm ⁻²) | V_{oc} (V) | FF | PCE (%) |
|---------|--------------------|---------------------------------|--------------|------|---------|
| P1DB | 1:4 ([60]PCBM) | 2.08 | 1.04 | 0.33 | 0.71 |
| | 1:3 ([70]PCBM) | 3.36 | 0.91 | 0.35 | 1.08 |
| P2DB | 1:3 ([70]PCBM) | 3.75 | 0.39 | 0.37 | 0.56 |
| P3DB | 1:4 ([60]PCBM) | 2.12 | 0.55 | 0.34 | 0.39 |
| | 1:3 ([70]PCBM) | 3.17 | 0.57 | 0.34 | 0.62 |

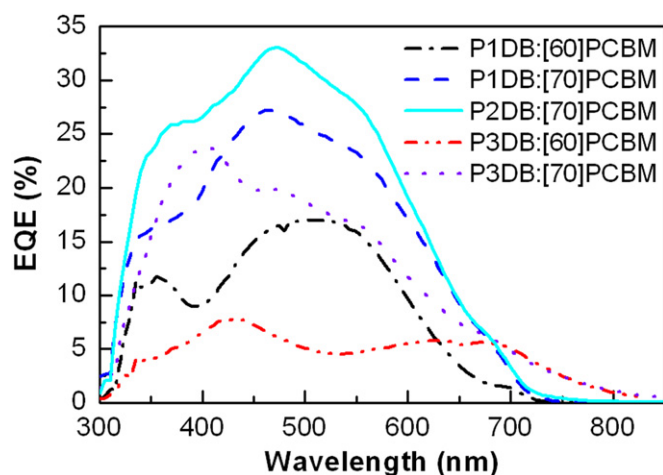


Fig. 4. The EQE profiles of the polymer solar cells.

from ODCB solution of P1DB:[70]PCBM showed a PCE of 1.08% with V_{oc} of 0.91 V and J_{sc} of 3.36 mA cm⁻² under AM 1.5G solar simulator (100 mW cm⁻²) conditions. P3DB had a promising absorption spectrum that peaked at around 700 nm and its EQE had a photoresponse up to ~800 nm, but the low V_{oc} limited its PCE. The molecular weights of the polymers were improved by using ODCB as the solvent instead of chloroform. These results indicate that ODCB is a promising solvent in the FeCl₃ oxidative polymerization for obtaining high molecular weight conjugated polymers.

Acknowledgments

We thank the Swedish Foundation for Strategic Research (SSF) for financial support through the Centre of Organic Electronics (COE).

References

- [1] G. Yu, J. Gao, J.C. Hummelen, F. Wudl, A.J. Heeger, Polymer photovoltaic cells: enhanced efficiencies via a network of internal donor-acceptor heterojunctions, *Science* 270 (1995) 1789–1791.
- [2] M. Helgesen, R. Sondergaard, F.C. Krebs, Advanced materials and processes for polymer solar cell devices, *J. Mater. Chem.* 20 (2010) 36–60.
- [3] F.C. Krebs, Fabrication and processing of polymer solar cells: a review of printing and coating techniques, *Sol. Energy Mater. Sol. Cells* 93 (2009) 394–412.
- [4] B. Kippelen, J.-L. Bredas, Organic photovoltaics, *Energy Environ. Sci.* 2 (2009) 251–261.
- [5] T. Ameri, G. Dennler, C. Lungenschmied, C.J. Brabec, Organic tandem solar cells: a review, *Energy Environ. Sci.* 2 (2009) 347–363.
- [6] E.G. Wang, L. Wang, L.F. Lan, C. Luo, W.L. Zhuang, J.B. Peng, Y. Cao, High-performance polymer heterojunction solar cells of a polysilafluorene derivative, *Appl. Phys. Lett.* 92 (2008) 033307/1–033307/3.
- [7] G. Li, V. Shrotriya, J.S. Huang, Y. Yao, T. Moriarty, K. Emery, Y. Yang, High-efficiency solution processable polymer photovoltaic cells by self-organization of polymer blends, *Nat. Mater.* 4 (2005) 864–868.
- [8] W.L. Ma, C.Y. Yang, X. Gong, K. Lee, A.J. Heeger, Thermally stable, efficient polymer solar cells with nanoscale control of the interpenetrating network morphology, *Adv. Funct. Mater.* 15 (2005) 1617–1622.
- [9] J. Hou, H.-Y. Chen, S. Zhang, G. Li, Y. Yang, Synthesis, characterization, and photovoltaic properties of a low band gap polymer based on silole-containing polythiophenes and 2,1,3-benzothiadiazole, *J. Am. Chem. Soc.* 130 (2008) 16144–16145.
- [10] J. Peet, J.Y. Kim, N.E. Coates, W.L. Ma, D. Moses, A.J. Heeger, G.C. Bazan, Efficiency enhancement in low-bandgap polymer solar cells by processing with alkane dithiols, *Nat. Mater.* 6 (2007) 497–500.
- [11] S.H. Park, A. Roy, S. Beaupre, S. Cho, N. Coates, J.S. Moon, D. Moses, M. Leclerc, K. Lee, A.J. Heeger, Bulk heterojunction solar cells with internal quantum efficiency approaching 100%, *Nat. Photonics* 3 (2009) 297–302.
- [12] J. Roncali, Synthetic principles for bandgap control in linear pi-conjugated systems, *Chem. Rev.* 97 (1997) 173–205.
- [13] A. Dhanabalan, J.K.J. van Duren, P.A. van Hal, J.L.J. van Dongen, R.A.J. Janssen, Synthesis and characterization of a low bandgap conjugated polymer for bulk heterojunction photovoltaic cells, *Adv. Funct. Mater.* 11 (2001) 255–262.
- [14] S.E. Shaheen, D. Vangeneugden, R. Kiebooms, D. Vanderzande, T. Fromherz, F. Padinger, C.J. Brabec, N.S. Sariciftci, Low band-gap polymeric photovoltaic devices, *Synth. Met.* 121 (2001) 1583–1584.
- [15] M.C. Scharber, D. Wuhlbacher, M. Koppe, P. Denk, C. Waldauf, A.J. Heeger, C.J. Brabec, Design rules for donors in bulk-heterojunction solar cells-towards 10% energy-conversion efficiency, *Adv. Mater.* 18 (2006) 789–794.
- [16] N. Blouin, A. Michaud, D. Gendron, S. Wakim, E. Blair, R. Neagu-Plesu, M. Belletete, G. Durocher, Y. Tao, M. Leclerc, Toward a rational design of poly(2,7-carbazole) derivatives for solar cells, *J. Am. Chem. Soc.* 130 (2008) 732–742.
- [17] L.M. Campos, A. Tontcheva, S. Günes, G. Sonmez, H. Neugebauer, N.S. Sariciftci, F. Wudl, Extended photocurrent spectrum of a low band gap polymer in a bulk heterojunction solar cell, *Chem. Mater.* 17 (2005) 4031–4033.
- [18] E. Bundgaard, F.C. Krebs, Low band gap polymers for organic photovoltaics, *Sol. Energy Mater. Sol. Cells* 91 (2007) 954–985.
- [19] E. Bundgaard, F.C. Krebs, Low-band-gap conjugated polymers based on thiophene, benzothiadiazole, and benzobis(thiadiazole), *Macromolecules* 39 (2006) 2823–2831.
- [20] M. Svensson, F.L. Zhang, S.C. Veenstra, W.J.H. Verhees, J.C. Hummelen, J.M. Kroon, O. Inganäs, M.R. Andersson, High-performance polymer solar cells of an alternating polyfluorene copolymer and a fullerene derivative, *Adv. Mater.* 15 (2003) 988–991.
- [21] E.G. Wang, M. Wang, L. Wang, C.H. Duan, J. Zhang, W.Z. Cai, C. He, H.B. Wu, Y. Cao, Donor polymers containing benzothiadiazole and four thiophene rings in their repeating units with improved photovoltaic performance, *Macromolecules* 42 (2009) 4410–4415.
- [22] A.P. Zoombelt, J. Gilot, M.M. Wienk, R.A.J. Janssen, Effect of extended thiophene segments in small band gap polymers with thienopyrazine, *Chem. Mater.* 21 (2009) 1663–1669.
- [23] D. Mühlbacher, M. Scharber, M. Morana, Z.G. Zhu, D. Waller, R. Gaudiana, C. Brabec, High photovoltaic performance of a low-bandgap polymer, *Adv. Mater.* 18 (2006) 2884–2889.
- [24] C. Soci, I.W. Hwang, D. Moses, Z. Zhu, D. Waller, R. Gaudiana, C.J. Brabec, A.J. Heeger, Photoconductivity of a low-bandgap conjugated polymer, *Adv. Funct. Mater.* 17 (2007) 632–636.
- [25] M.R. Andersson, D. Selse, M. Berggren, H. Järvinen, T. Hjertberg, O. Inganäs, O. Wennerström, J.E. Österholm, Regioselective polymerization of 3-(4-octylphenyl)thiophene with FeCl₃, *Macromolecules* 27 (1994) 6503–6506.
- [26] M. Jayakannan, P.A. Van Hal, R.A.J. Janssen, Synthesis and structure-property relationship of new donor-acceptor-type conjugated monomers and polymers on the basis of thiophene and benzothiadiazole, *J. Polym. Sci. Polym. Chem.* 40 (2002) 251–261.
- [27] W. Yue, Y. Zhao, H.K. Tian, D. Song, Z.Y. Xie, D.H. Yan, Y.H. Geng, F.S. Wang, Poly(oligothiophene-alt-benzothiadiazole): tuning the structures of oligothiophene units toward high-mobility "black" conjugated polymers, *Macromolecules* 42 (2009) 6510–6518.
- [28] D.L. Vangeneugden, D.J.M. Vanderzande, J. Salbeck, P.A. van Hal, R.A.J. Janssen, J.C. Hummelen, C.J. Brabec, S.E. Shaheen, N.S. Sariciftci, Synthesis and characterization of a poly(1,3-dithienylisothianaphthene) derivative for bulk heterojunction photovoltaic cells, *J. Phys. Chem. B* 105 (2001) 11106–11113.
- [29] M.S.A. Abdou, X.T. Lu, Z.W. Xie, F. Orfino, M.J. Deen, S. Holdcroft, Nature of impurities in pi-conjugated polymers prepared by ferric-chloride and their effect on the electrical-properties of metal-insulator-semiconductor structures, *Chem. Mater.* 7 (1995) 631–641.
- [30] Y. Zhu, R.D. Champion, S.A. Jenekhe, Conjugated donor acceptor copolymer semiconductors with large intramolecular charge transfer: synthesis, optical properties, electrochemistry, and field effect carrier mobility of thienopyrazine-based copolymers, *Macromolecules* 39 (2006) 8712–8719.
- [31] K.G. Jørgensen, W.J.D. Beenke, Y. Zaushitsyn, A. Yartsev, M. Andersson, T. Pullerits, V. Sundström, The electronic states of polyfluorene copolymers with alternating donor-acceptor units, *J. Chem. Phys.* 121 (2004) 12613–12617.
- [32] A.P. Zoombelt, M. Fonrodona, M.M. Wienk, A.B. Sieval, J.C. Hummelen, R.A.J. Janssen, Photovoltaic performance of an ultrasmall band gap polymer, *Org. Lett.* 11 (2009) 903–906.
- [33] M.M. Wienk, J.M. Kroon, W.J.H. Verhees, J. Knol, J.C. Hummelen, P.A. van Hal, R.A.J. Janssen, Efficient methano[70]fullerene/MDMO-PPV bulk heterojunction photovoltaic cells, *Angew. Chem. Int. Ed.* 42 (2003) 3371–3375.
- [34] F.L. Zhang, J. Bijleveld, E. Perzon, K. Tvingstedt, S. Barrau, O. Inganäs, M.R. Andersson, High photovoltage achieved in low band gap polymer solar cells by adjusting energy levels of a polymer with the LUMOs of fullerene derivatives, *J. Mater. Chem.* 18 (2008) 5468–5474.